

Spin dynamics study of magnetic molecular clusters by means of Mössbauer spectroscopy

L. Cianchi,¹ F. Del Giallo,¹ and G. Spina²¹*Istituto di Ricerca sulle Onde Elettromagnetiche, CNR, Firenze via Panciatichi 64, 50127 Firenze, Italy*²*Dipartimento di Fisica, Associato INFN, Università di Firenze, via G. Sansone, 50019 Sesto Fiorentino (FI), Italy*

W. Reiff

Chemistry Department, Northeastern University, Boston, Massachusetts 02115

A. Caneschi

Department of Chemistry, Università di Firenze, Via Maragliano 75, I-50144 Firenze, Italy

(Received 26 July 2001; published 16 January 2002)

Spin dynamics of the two magnetic molecular clusters Fe₄ and Fe₈, with four and eight Fe(III) ions, respectively, was studied by means of Mössbauer spectroscopy. The transition probabilities W 's between the spin states of the ground multiplet were obtained from the fitting of the spectra. For the Fe₄ cluster we found that, in the range from 1.38 to 77 K, the trend of W 's versus the temperature corresponds to an Orbach's process involving an excited state with energy of about 160 K. For the Fe₈, which, due to the presence of a low-energy excited state, could not be studied at temperatures greater than 20 K, the trend of W 's in the range from 4 to 18 K seems to correspond to a direct process. The correlation functions of the magnetization were then calculated in terms of the W 's. They have an exponential trend for the Fe₄ cluster, while a small oscillating component is also present for the Fe₈ cluster. For the first of the clusters, τ vs T (τ is the decay time of the magnetization) has a trend which, at low temperatures ($T < 15$ K), corresponds to an Arrhenius law with a potential barrier of the order of the energy difference between the states $|M|=5$ and $M=0$ (≈ 7 K). Instead, for $T > 15$ K, τ follows the trend of W^{-1} . For the Fe₈, τ follows an Arrhenius law, but with a prefactor which is smaller than the one obtained susceptibility measurements.

DOI: 10.1103/PhysRevB.65.064415

PACS number(s): 67.57.Lm, 61.46.+w, 87.64.Pj

I. INTRODUCTION

In the last decade the magnetic properties of Fe₄ and Fe₈ molecular clusters,^{1,2} with four and eight Fe(III) ions (Figs. 1 and 2), respectively, have aroused much interest and have been extensively studied from both a theoretical and an experimental point of view. The ground state of these clusters was determined by using different experimental techniques such as susceptibility measurements,^{1,3} high field EPR,^{4,5} inelastic neutron scattering (INS),^{6,7} and the spin Hamiltonian parameters are now fairly well known.

The two clusters have ground states with $S=5$ and 10, respectively, and a prevalently axial magnetic anisotropy. Moreover, a transverse component is present in both clusters. However, for Fe₄, it is small and, in certain cases, negligible. Conversely, for Fe₈, the transverse component of the anisotropy strongly perturbs the spin states.

Many studies have dealt with the quantum tunneling of the magnetization.⁸⁻¹⁰ This phenomenon is possible due to the presence of the axial anisotropy, which splits the ground spin multiplet into S Kramer's doublets $|S, \pm M\rangle$ plus the singlet $|S, 0\rangle$. The doublet $|S, \pm S\rangle$ has the lowest energy, and at very low temperatures is the only doublet populated. The tunnel effect consists of coherent jumps between the two states of the doublet. As the temperature increases, doublets of higher and higher energies are populated and the interactions of the spin with the vibrational freedom degrees of the cluster produce transitions between doublets. The spin dynamics is then characterized by these transitions and by the tunnel effect inside the doublets.

In this paper, a Mössbauer study of the spin dynamics in

these two clusters, as a function of the temperature, is presented. We obtained the transition probabilities between the spin states from the fitting of the Mössbauer spectra. Moreover, the tunneling frequencies were evaluated by means of perturbation theory, starting from the spin Hamiltonian parameters present in the literature. These parameters were then kept free, and their values were determined in order to optimize the spectrum fits. Finally, the correlation function of the magnetization was calculated from the transition

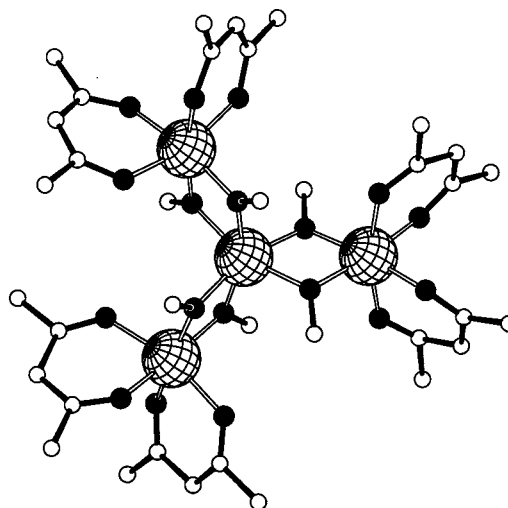


FIG. 1. Schematic structure of the Fe₄ cluster. Large spheres represent Fe(III) ions; black and white circles denote oxygen and carbon atoms, respectively. Hydrogen atoms are not indicated.

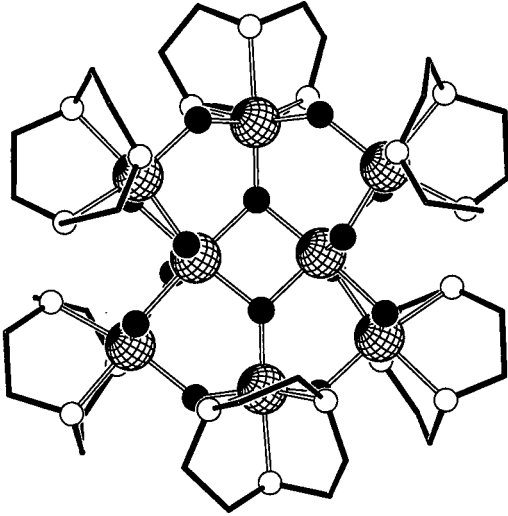


FIG. 2. Schematic structure of the Fe8 cluster. Large spheres represent Fe(III) ions; black and white circles denote oxygen and nitrogen atoms, respectively. Finally, carbon atoms are at the vertices of the black lines. Hydrogen atoms are not indicated.

probabilities between the spin states and the tunneling frequencies.

II. EXPERIMENT

The Mössbauer spectra were determined using a conventional constant acceleration spectrometer operated in a multichannel scaling mode. The gamma ray source consisted of a fresh 51 mCi of ^{57}Co in a rhodium metal matrix, that was maintained at ambient temperature. The spectrometer was calibrated using a 6- μm -thick natural abundance iron foil. Isomer shifts are reported relative to the center of the magnetic hyperfine pattern of the latter foil taken as zero velocity. The linewidths of the innermost pair of DMI transitions equal to 1 of the latter Zeeman pattern were reproducibly determined to be 0.214 mm s^{-1} . The sample temperature variation was achieved using a standard exchange gas liquid helium cryostat (Cryo Industries of America, Inc.), with temperature measurement and control based on silicon diode thermometry in conjunction with a 10- μA excitation source (Lakeshore Cryotronics, Inc). The spectra were initially fit to unconstrained Lorentzians using the program ORIGIN (Microcal Software, Inc.)

III. THEORY OF THE SPECTRUM FIT

For a cluster with N Fe^{+3} ions, the electronic states are obtained by coupling the Fe^{+3} ion spins ($s=5/2$). Thus 6^N cluster spin states are obtained. For Fe4 and Fe8, we have 1296 and 1 679 616 spin states, respectively. Detailed calculations for the two clusters were reported in Refs. 1 and 2. These were based on the Heisemberg antiferromagnetic Hamiltonian, and tested using susceptibility measurements. Since we are mainly interested in spin dynamics at low temperatures, only the ground spin states of the Fe4 and Fe8 clusters will be considered. They have values of $S=5$ and 10, respectively.

The main terms of spin Hamiltonian for the ground state have the same form for both clusters,

$$H_s = DS_z^2 + \frac{E}{2}(S_+^2 + S_-^2) + H_{h.o.}, \quad (3.1)$$

where $H_{h.o.}$ denotes fourth-order terms in the spin components. The measurements of the D and E parameters, as well as the fourth-order parameters that have not been explicitly written here, were performed by means of high-field electron paramagnetic resonance (HF-EPR)^{2-5,10} and inelastic neutron scattering (INS).^{6,7} For Fe4, these measurements are complicated as three different isomers are present in the single-crystal samples. However, the two techniques give practically the same values for the axial parameter D . For the three isomers AA, AB, and BB (see Ref. 4), the values of this parameter were -0.29 , -0.27 and -0.25 K, respectively. On the other hand, very different values were obtained for E . For example, for the AA isomer, HF-EPR and INS gave $E = -0.014$ and -0.029 K, respectively. However, since both the E values are much smaller than the D values, the $S=5$ ground state consists approximately of five Kramer's quasidegenerate doublets $|5, \pm M\rangle$, with the $|5, \pm 5\rangle$ doublet having the lowest energy, plus the singlet $|5, 0\rangle$.

Now, let us consider the Fe8 cluster. For this cluster, INS gave $D = -0.29$ K, against the value of -0.275 K obtained from the EPR, while both techniques gave the same value of E : $E = -0.047$ K. In this case, by diagonalizing H_s in the space of the ground spin states $|10, M\rangle$, we obtained the states shown in Fig. 3. We can see that the six quasidegenerate lowest doublets do not differ much from the ones corresponding to the axial term of the spin Hamiltonian H_s . Conversely, as far as the nine highest singlets are concerned, we have a strong mixing of the states with different M 's, due to the transverse term of H_s .

As mentioned above, the state $|5, \pm M\rangle$ of Fe4 and the states $|10, \pm M\rangle$ for $|M| \geq 5$ of Fe8 are almost degenerate. Their energy differences ν_M (in unit s^{-1}), which are due to the transverse terms of H_s , represent the so-called *quantum tunneling frequencies*: i.e., for a given M , the frequencies of the coherent $M \leftrightarrow -M$ jumps.

It will be useful to evaluate the ν_M 's as functions of M and $E/|D|$. In order to do this, it is appropriate to use the Brillouin-Wigner perturbation theory, which gives the effective Hamiltonian¹¹

$$H_{eff} = H + \sum_{\mu} \frac{H|\mu\rangle\langle\mu|H}{E - E_{\mu}^0} + \sum_{\mu, \nu} \frac{H|\mu\rangle\langle\mu|H|\nu\rangle\langle\nu|H}{(E - E_{\mu}^0)(E - E_{\nu}^0)} + \dots, \quad (3.2)$$

where H_{eff} is the Hamiltonian which couples the states M and $-M$ of the Kramer's doublets. Here we consider only the term of H_{eff} which gives the first non-null contributions to $\langle M|H_{eff}| -M\rangle$, and puts $E = E_M^0$.

H consists of terms of the spin Hamiltonian containing S_+ and S_- operators. The largest term is obviously the rhombic term $(E/2)(S_+^2 + S_-^2)$. In order of magnitude, the following term is $(C/2)(S_+^4 + S_-^4)$ Ref. 4. For Fe4, an estimate of C was obtained from HF-EPR, which gave $C \approx 6$

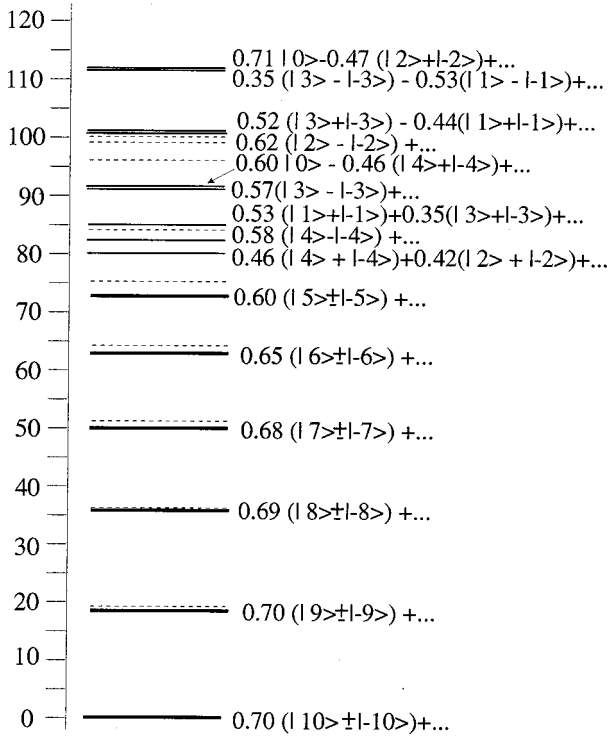


FIG. 3. Level scheme of the ground state of the Fe8 cluster obtained from the INS data. The six lowest levels (bold lines) are quasidegenerate Kramer's doublets. The nine highest levels are singlets with $\langle M \rangle = 0$. The dashed lines denote the levels corresponding to the axial term of H_s . The scale on the left gives the energies in the unit $|D|$. Only the larger terms of the states are written.

$\times 10^{-5}$ K. For Fe8, from INS we have $C = 8.6 \times 10^{-6}$ K. By using Eq. (3.2), we can verify that for the Fe8 the fourth-order term is quite negligible with respect to the rhombic term. Conversely, for Fe4, the contributions of the two terms are comparable. For the sake of simplicity and in order to reproduce the line shape of the Mössbauer spectra, we will assume that the tunneling frequencies are determined only by the rhombic term of H_s for both the clusters; however, for Fe4, E/D will be treated as an iterative parameter.

By using Eq. (3.2) the following expression for ν_M is obtained:

$$\nu_M = F(M) \left(\frac{E}{2|D|} \right)^M \frac{|D|}{h}, \quad (3.3)$$

where $F(M)$'s are rational numbers that are independent of E and D . Their value for the two clusters are reported in Table I.

In order to determine the shapes of the Mössbauer spectra, in addition to the static interactions between electrons and nuclei of ^{57}Fe , we have to take into account the dynamics of the spins which produce fluctuations in the hyperfine field. These fluctuations have a twofold origin: first, as mentioned above, the quantum tunneling of the magnetization, which causes inversions of the hyperfine field with frequencies ν_M ; second, the interactions with the vibrational freedom degrees of the cluster, which, we assume, cause transitions $M \leftrightarrow M - 1$.¹² The corresponding dynamic spin Hamiltonian can be

TABLE I. Values of the quantity $F(M)$ corresponding to the ground-state doublets of the two clusters.

	M	$F(M)$	M	$F(M)$	
Fe4	1	60	Fe8	5	147804
	2	420		6	118244
	3	630		7	55838
	4	315		8	15384
	5	1575/32		9	2284
			10	140	

written in the form: $H_d = FA(S_x, S_y, S_z)$, where F is an operator acting on the vibrational freedom degrees, and is usually assumed to have an order of magnitude of H_d . Moreover, A is a dimensionless operator. If F has a magnetic origin, A is simply S_x or S_y or, equivalently, a linear combination of these. In fact, since H_d has to be an even operator to time inversion, as F is an odd operator, A also has to be odd. Instead, if F has an electric origin, F is an even operator and A also has to be even. For instance, $A = \frac{1}{2}(S_x S_z + S_z S_x)$.

The probabilities per unit time for the transitions $|S, M\rangle \leftrightarrow |S, M-1\rangle$ read¹³

$$W_{M, M-1} = |\langle M | A | M-1 \rangle|^2 J(\omega_{\Delta M}),$$

$$W_{M-1, M} = W_{M, M-1} \exp(\omega_{\Delta M}/T), \quad (3.4)$$

where $\omega_{\Delta M}$ is the difference between the energies (in unit K) of the two states and $J(\omega)$ is the Fourier transform of the correlation function of F . We have assumed that the correlation time of F is much shorter than D^{-1} . In this case we have

$$J = \int_{-\infty}^{\infty} \langle F(0)F(t) \rangle dt \quad (3.5)$$

i.e., J is the same for all the transitions.

A. Fe4 cluster

The spectrum shapes will be evaluated by using Blume's stochastic theory, as described in Ref. 12, where only the thermal motion of the spins was studied in the 10–60-K temperature range. With respect to Ref. 12, tunnelings $M \leftrightarrow -M$ —the frequencies of which we denoted above by ν_M —were considered here, and spectra at lower temperatures, down to 1.38 K, were collected. By taking all this into account, the spectrum shape corresponding to one of the sites can be expressed in terms of eigenvectors and eigenvalues of a complex non-Hermitian matrix—Blume's matrix—which in this case has dimensions of 88×88 .

The following fitting hyperfine parameters were assumed: the quadrupolar parameters and the isomer shifts at the three nonequivalent Fe sites, and the hyperfine field at the ^{57}Fe nuclei for the state $s_z = 5/2$ (the same for the three sites). Finally, as far as the relaxation parameters are concerned, we used the probability per unit time $W = W_{5,4}$ and the ratio E/D . Moreover, as D value was assumed the weighed average of the values corresponding to the three isomers.

TABLE II. Tunneling frequencies for the Fe8 cluster.

M	5	6	7	8	9	10
$\nu_M(\text{Hz})$	3.6×10^9	2.4×10^8	9.6×10^6	2.2×10^5	2.8×10^4	14.8

B. Fe8 cluster

In this case, in order to calculate the spectrum shapes, we met a twofold difficulty. First, the energy of the $S=9$ state is not precisely known, but should be of the order of the ground-state energy range ($\approx 100D = 27.5$ K).¹ The calculation of the spectra, disregarding the excited levels, is then corrected only for $T \ll 30$ K. Second, the Blume matrix would have the order of 168×168 , so that, also by taking into account the large number of parameters, the spectrum fittings occupy a rather long computation time.

However, a simplified theoretical approach can be used, which is based on the particular structure of the ground-level states. As we have seen above, these states can be ideally divided into two groups: the first group consists, with a good approximation, of the six lowest Kramer's doublets $|10, \pm M\rangle$ (for M from 5 to 10). The second group consists of the other nine states (singlets). Since in every one of these states M has an average value of zero, their Mössbauer-spectrum contribution does not have a magnetic structure and will be the same for all of them, apart from the absorption area. In order to reproduce the experimental spectra, we will then consider the nine states as a single fictitious state $|f\rangle$, the occupation of which is the sum of the occupations of the nine states. This fictitious state will be assumed to be coupled with the first group of states through the interaction with the thermal bath. The corresponding transition probabilities are evaluated by the relation

$$W_{M,f} = \sum_{i=1}^9 W_{M,i} \propto \sum_{i=1}^9 |\langle 10, M | A | \psi_i \rangle|^2, \quad (3.6)$$

where $\{|\psi_i\rangle\}$ ($i=1$ to 9) are the states of the second group. Moreover,

$$W_{f,M} = \sum_{i=1}^9 W_{M,i} \exp\{\omega_{i,M}/T\}, \quad (3.7)$$

where $\omega_{i,M}$ is the energy difference (in K) between the $|\psi_i\rangle$ and $|10, M\rangle$ states. By using this simplified model, the order of the Blume's matrix is reduced from 168×168 to 104×104 .

For the first group of states, we assume the tunneling frequencies to be known. To be precise, these frequencies will be evaluated from the EPR or INS values of D and E . Their values are reported in Table II.

As far as the hyperfine magnetic field is concerned, it is very cumbersome to correlate fields at different sites with the cluster spin states, as we could do for the Fe4 cluster. In fact, in the case of Fe8, the relation between the spin of the cluster and the spin of the single iron ions depends on four exchange parameters, the values of which are not exactly known. We shall then consider the magnetic fields at the three sites for

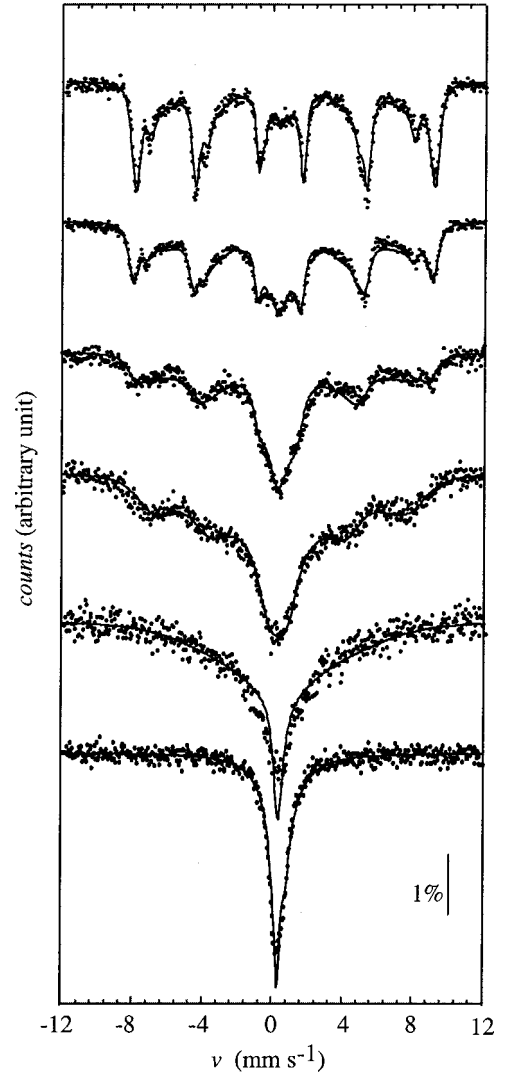


FIG. 4. Mössbauer spectra of the Fe4 cluster at the temperatures of (starting from the top) 1.38, 4.25, 12.5, 25.7, 45, and 77 K.

$M=10$ as fitting parameters, and evaluate the B_M field for the spin state M by scaling in proportion to M :

$$B_M = \frac{M}{10} B_{M=10}. \quad (3.8)$$

In a previous work, in which a spectrum at 2 K in the presence of an applied field of 0.22 T was reported,³ the quadrupolar splitting was found to be negligible. However, here, in order to evaluate the spectra, we will assume the presence at each site of an EFG having axial symmetry, with the axis parallel to the hyperfine field.

IV. RESULTS OF EXPERIMENTS

A. Fe4 cluster

The Mössbauer spectra, together with their fits, are shown in Fig. 4. The quadrupolar parameters (Δ_Q and η) ($\Delta_Q = e^2 V_{zz} Q/2$) and the isomer shift (IS) at the three sites and the hyperfine field corresponding to $s_z = 5/2$ were obtained from

TABLE III. Hyperfine parameters obtained from the fitting of lowest-temperature spectrum for the Fe4.

Parameter	Central site	Apical site	Lateral sites
Δ_Q (mm s ⁻¹)	-0.55 ± 0.3	0.11 ± 0.1	-0.32 ± 0.06
IS ^a (mm s ⁻¹)	0.38 ± 0.05	0.37 ± 0.07	0.42 ± 0.04

^aValues referring to metallic iron.

the fit of the spectra at 1.38 K. At this temperature, the relaxation effects on the spectrum shape are negligible, so that the spectrum contains maximum information about the hyperfine parameters. An estimate of the EFG showed that one of the principal axes of this tensor has a direction that is practically perpendicular to the iron containing plane, for all three sites.¹² In the fitting, we assumed the z axis to be in this direction, and we found that the η values at all sites were much greater than 1. That is, the corresponding maximum EFG components are directed in the iron plane. The values of Δ_Q and the IS are reported in Table III. We note that the Δ_Q absolute value for the apical site is smaller than for the central site. Conversely, on the basis of the symmetry of the two sites, it would seem that the central iron should experience an EFG smaller than the apical iron. Moreover, the hyperfine field corresponding to $s_z = 5/2$ —the same at all the sites—was $B_{max} = 56.7 \pm 0.6$ T.

As far as the spin Hamiltonian parameters are concerned, we first performed spectrum fittings using the weighed average of INS or EPR values of the three isomers. However, very poor results were obtained ($\chi^2 > 3100$). Then E/D and $|D|$ were kept free. The best fit of the spectrum at 1.38 K was obtained for $|D| = 0.20 \pm 0.05$ and E/D in the (from 1 to 2) 10^{-3} range. The $|D|$ value is of 20–30% smaller than the INS or EPR values, while E/D is smaller by one order of magnitude.

In order to establish the presence of quantum tunneling, fitting of the spectrum at 1.38 K with $E=0$ was carried out. However, the central part of the spectrum was poorly reproduced and χ^2 passed from 1770 (with E/D free parameter) to 2186 (with $E=0$).

We observed that, although the spectra were fitted by using a dynamic Hamiltonian corresponding to both magnetic and electric fluctuating fields, we obtained satisfactory results only with the former. For instance, for the 4.25-K spectrum, the best fit obtained with the second Hamiltonian had $\chi^2 = 3864$.

As we can see in Fig. 4, 45- and 77-K spectra are not fitted quite well in the central region. This is probably why we did not take into account the contribution from the excited $S=4$ spin state, which, at these temperature, should be of about 15% and 30%, respectively.

The values of $W(T)$ obtained with the first Hamiltonian are reported in Table IV, together with the χ^2 values. A good fit of the trend of $W(T)$ is given by the function

$$W(T) = (9885 \pm 564) \exp[-(161 \pm 4)/T]. \quad (4.1)$$

This is the characteristic trend of the Orbach mechanism involving an excited state with an energy of about 160 K.

TABLE IV. Transition probabilities per unit time for the transition $M=5 \rightarrow M=4$ of Fe4. Values obtained from the fitting of the spectra. χ^2 values are also shown.

T (K)	$W(T)$ (MHz)	χ^2
1.38	2.0 ± 0.1	1171
4.25	3.3 ± 0.1	2488
12.5	7.5 ± 0.3	1128
25.7	37.0 ± 1	1016
45.0	267.0 ± 5	1428
77.0	1198 ± 40	1022

States of this energy are definitely present, since the energy difference between the ground $S=5$ state and the top $S=10$ state is about 1200 K ($J \approx 30$ K), with 1296 spin states shared in this range.

On the other hand, up to now neither the microscopic relaxation mechanism nor the vibrational mode of the cluster is known. However, on the basis of result (4.1), we can hypothesize that a 160-K centered peak of the vibrational-state density is present, and this could account for the $W(T)$ trend observed. Nevertheless, further studies are necessary in order to clarify this issue.

B. Fe8 cluster

In this case, only three spectra at temperatures lower than 20 K were collected (Fig. 5). The reason for this is that at higher temperatures the contribution of the excited spin states are not negligible. The spin Hamiltonian parameters were fixed at the INS values ($D = -0.29$ K and $E = 0.047$ K). However, almost equivalent fittings were obtained by allowing D to change in the range from -0.27 to -0.30 K.

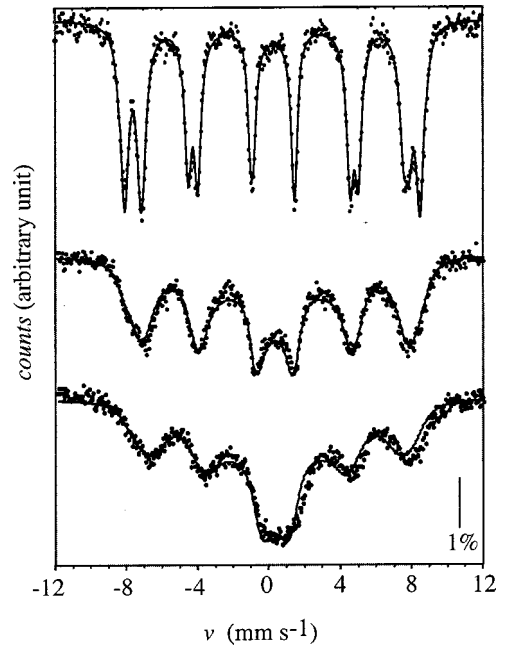


FIG. 5. Mössbauer spectra of the Fe8 cluster at temperatures of (starting from the top) 4.2, 11, and 18 K.

TABLE V. Hyperfine parameters obtained from the fitting of the Fe8 lowest temperature spectrum.

Parameter	Central sites	Apical sites	Lateral sites
Δ_Q (mm s ⁻¹)	0.13±0.01	-0.11±0.02	0.057±0.002
IS ^a (mm s ⁻¹)	0.25±0.01	0.36±0.01	0.24±0.01
B_{max} (T)	47.3±0.1	47.9±0.1	53.1±0.1

^aValues referred to metallic iron.

Like the procedure followed for the Fe4 cluster, the hyperfine parameters were obtained from the spectrum at the lowest temperature (4.2 K), which presents a well-resolved hyperfine structure. The values of these parameters are reported in Table V.

In this case, differently from that for the Fe4 cluster, both the dynamic spin Hamiltonians gave satisfactory fittings. The values of W for the three temperatures considered together with the χ^2 values are reported in Table VI. Similar to the Fe4 cluster, the increase of χ^2 with the temperature is probably due to the excited-state contributions to the spectra.

We see that $W^{(1)}(T)$ has a linear trend with the temperature. To be precise, the best fit gave (in MHz)

$$W^{(1)}(T) = (2.2 \pm 0.1)T, \quad (4.2)$$

which is a characteristic trend of the direct relaxation process. Also the trend of $W^{(2)}(T)$ is approximately linear with the temperature. The best linear fit is

$$W^{(2)}(T) = (-12.5 \pm 8.5) + (4.5 \pm 0.6)T. \quad (4.3)$$

But the power law $W^{(2)}(T) = 1.2T^{1.4}$ gives a better fit of the data. However, whether this trend could be characteristic of a direct process is fairly questionable.

V. DYNAMICS OF THE MAGNETIZATION

Let us suppose a magnetic field is applied to a crystalline sample of noninteracting magnetic clusters in the direction of the anisotropy axis. The solid will then present a magnetization parallel to the applied field, which is given by the sum of the magnetic moments of the clusters. If the magnetic field is slowly reduced to zero, at $T=0$ the magnetization can persist for a long time. In fact, at $T=0$ the magnetization can be canceled only by quantum tunneling, that is, by a transition between the two states $|m\rangle$ and $|-m\rangle$ —corresponding to

TABLE VI. Transition probabilities per unit time for the transition $M=10 \rightarrow M=9$ of Fe8. Values obtained from the spectrum fittings by using the two different interaction Hamiltonians described in the text (see notes). χ^2 values are also shown.

T (K)	$W(T)^{(1)a}$ (MHz)	χ^2	$W(T)^{(2)b}$ (MHz)	χ^2
4.2	8.2±0.6	1050	9.1±0.7	1103
11.0	23.2±1.3	1389	31.3±2.2	1856
18.0	40.2±2.5	2272	70.8±3.0	2610

^aValues obtained with $H = FS_x$.

^bValues obtained with $H = (F/2)(S_x S_z + S_z S_x)$.

opposed magnetic moments—which is due to an internal interaction H_{eff} coupling the two states: $\langle m | H_{eff} | -m \rangle \neq 0$. Then, if the cluster is in the state $|m\rangle$ at a time $t=0$, its state will jump, in a coherent way, from $|m\rangle$ to $|-m\rangle$, and vice versa, with frequency $\nu_T = 2\langle m | H_{eff} | -m \rangle / h$. This phenomenon is called the *quantum tunneling of the magnetization*. Usually, ν_T is very small because the coupling between the two states is weak. However, as the temperature increases, the tunneling frequency becomes higher and higher. This means that the phenomenon is mainly determined by interactions of the cluster magnetic moments with the thermal bath. We are now considering a *thermally assisted tunnel effect*.

The characteristic times of the thermally assisted tunnel effect can be obtained by evaluating the correlation function for the magnetization I ,

$$\langle I(0)I(t) \rangle = \text{Tr}\{\rho I(0)\exp(iHt)I(0)\exp(-iHt)\}_{M,b}, \quad (5.1)$$

where $\{ \}_{M,b}$ means that the trace is made on a complete set of states of the system cluster plus thermal bath, ρ is the density operator, and H is the total Hamiltonian

$$H = H_1 + H_2 + H_{12}, \quad (5.2)$$

in which H_1 and H_2 are the Hamiltonians of the cluster and the thermal bath, respectively, and H_{12} is the interaction Hamiltonian. Since we are interested in the evolution of the cluster state, and its interaction with the bath can be supposed to be weak, we can describe the action of the latter as a stochastic interaction. This can be done by projecting the state of the entire system onto the cluster-spin space.¹⁴ In this approximation, we have

$$\langle I(0)I(t) \rangle = \text{Tr}\{\rho_M I(0)\langle \exp(iH^x t) \rangle_b I(0)\}_{M}, \quad (5.3)$$

where the trace is now made on the spin states $|S, \pm M\rangle$ of the cluster. Moreover, we have written the temporal evolution operator in terms of the Liouville operator corresponding to the Hamiltonian H . In the Appendix, the calculation of $\langle I(0)I(t) \rangle$ is developed in terms of the probabilities per unit time for the transitions between the ground spin states, which have been determined by means of Mössbauer spectroscopy.

In summary, the results are as follows. Let us consider a Liouville space¹⁵ of the spin states $|S, M\rangle$. Each Liouville state is labeled with two components M and M' of S , and will be denoted $|M, M'\rangle$. The matrix \mathbf{L} of the operator $-iH_{eff}^x + R$ have to be built on this space, where R is the operator describing the stochastic interaction of the cluster with the thermal bath, and H_{eff}^x is the Liouville operator of H_{eff} . The non-null elements of matrix of H_{eff}^x and R are given by

$$\begin{aligned} \langle M, M | H_{eff}^x | -M, M \rangle &= \langle -M, M | H_{eff}^x | M, M \rangle = \nu_M, \\ \langle M, M | H_{eff}^x | M, -M \rangle &= \langle M, -M | H_{eff}^x | M, M \rangle = -\nu_M, \end{aligned} \quad (5.4)$$

and

$$\langle M, M | R | M', M' \rangle = \begin{cases} \sum_{M'' (\neq M)} W_{M, M''} & \text{for } M = M' \\ -W_{M, M'} & \text{for } M \neq M'. \end{cases} \quad (5.5)$$

Since \mathbf{L} is not Hermitian, its eigenvectors \mathbf{U}_α are different from the eigenvectors \mathbf{V}_α of \mathbf{L}^\dagger . If a_α 's denote the autovalues of \mathbf{L} and we consider the matrix $\mathbf{P}(t)$ defined by

$$\mathbf{P}(t) = \sum_{\alpha} \mathbf{U}_\alpha \mathbf{V}_\alpha^\dagger \exp(-a_\alpha t), \quad (5.6)$$

we have

$$\langle I(0)I(t) \rangle = \sum_{M, M'} p_M P_{M', M}(t) M M', \quad (5.7)$$

where p_M is the probability that the cluster is in the state M , and $P_{M', M}(t)$ are the elements of the line (M', M') and of the column (M, M) of \mathbf{P} .¹⁶

A. Fe4 cluster

Since we have obtained $E \ll |D|$ from the fittings of the Mössbauer spectra, in order to evaluate the correlation function of the magnetization, we can consider only the cluster-thermal bath interaction, disregarding the tunneling effect. The trend of $\langle I(0)I(t) \rangle$ is reproduced, with very good approximation for all of the temperatures considered, by means of an exponential function

$$\langle I(0)I(t) \rangle \propto \exp\left(-\frac{t}{\tau}\right), \quad (5.8)$$

where the decay constant τ depends on the temperature.

For very low temperatures, the thermally assisted tunneling of the magnetization consists of a stochastic process in which, starting from one of the two $|M|=5$ states, the cluster climbs as far as the $M=0$ state and then descends to the other $|M|=5$ state. The order of the matrix \mathbf{P} is then of 11×11 . In this case, τ is expected to be well represented by an Arrhenius law that concerns the overcoming of a potential Δ :

$$\tau = \tau_0 \exp(\Delta/T). \quad (5.9)$$

However, as the temperature increases, this simple law disagrees with the experimental behavior. For instance, for $T > \Delta$, according to the Arrhenius law, τ should keep the constant value τ_0 , while the experimental data show a greater and greater decrease in τ as the temperature increases. This is why, according to the trend of W obtained from the Mössbauer data, the steps between the subsequent states M became faster and faster. Taking these considerations into account, we have fitted the trend of τ^{-1} with the temperature by a function of the form (see Fig. 6)

$$\tau^{-1} = [\tau_0^{-1} + a \exp(-b/T)] \exp(-\Delta/T). \quad (5.10)$$

The value obtained for the parameters are

$$\tau_0^{-1} = (1.9 \pm 0.4) 10^7 \text{ s}^{-1},$$

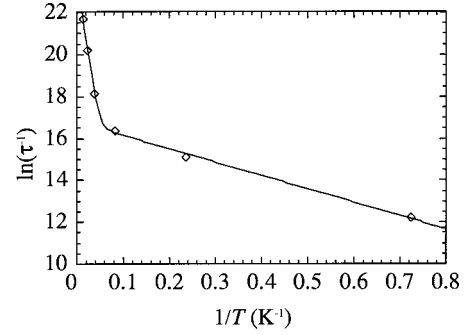


FIG. 6. Plot of $\ln(\tau^{-1})$ vs T^{-1} . The experimental points are obtained as described in the text. The full line represents the curve fit obtained with the function defined by Eq. (5.10).

$$a = (1.6 \pm 0.5) 10^{10} \text{ s}^{-1},$$

$$b = (138 \pm 13) \text{ K},$$

$$\Delta = (6.4 \pm 0.5) \text{ K}.$$

We see that, at low temperatures ($T < 15$ K), the second term in square brackets of Eq. (5.10) can be disregarded, and that the trend of τ^{-1} is well described by an Arrhenius law with Δ of order of the energy difference between the levels $M=0$ and $|M|=5$, i.e., 7 K. For high temperatures ($T > 20$ K), the exponential $\exp(-\Delta/T)$ is near unity, and the first term in square brackets becomes negligible with respect to the second. The trend of τ^{-1} is then similar to the trend of W .

B. Fe8 cluster

Calculation of the correlation function is more complicated than for Fe4, because now the tunneling effect cannot be disregarded. The trend of $\langle I(0)I(t) \rangle$ can be reproduced by means of an exponential function plus an oscillating component (Fig. 7), at all of the temperatures considered. By fitting the decay constant τ^{-1} as a function of the tempera-

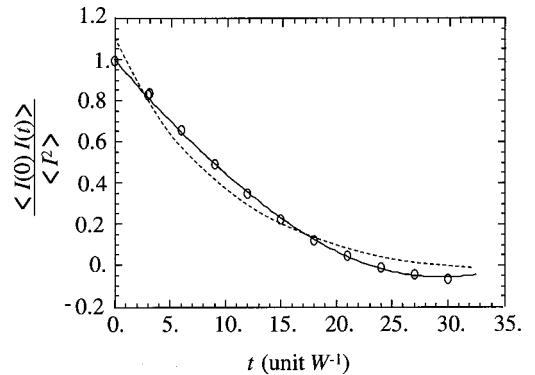


FIG. 7. Correlation function of the magnetization vs time, for the Fe8 cluster at a temperature of 4.2 K. The experimental points are obtained as described in the text. The full line represents the curve fit obtained with an exponential plus an oscillating function. The dashed line is the fit obtained with the exponential function alone.

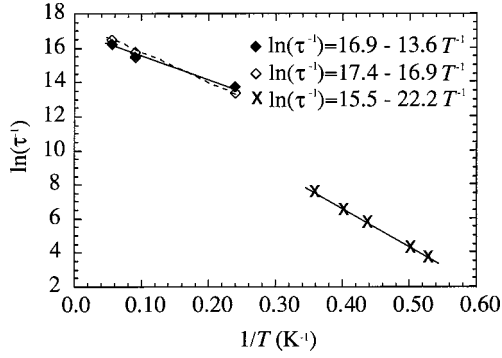


FIG. 8. Plot of $\ln(\tau^{-1})$ vs T^{-1} for the Fe8 cluster. Crosses refer to susceptibility data; full and empty diamonds refer to Mössbauer data corresponding to $H=FS_x$ and $H=F(S_xS_z+S_zS_x)$, respectively.

ture by means of a simple Arrhenius law, for $H=FS_x$ and $H=F(S_xS_z+S_zS_x)$, respectively, we obtain

$$\tau_0^{-1} = (1.6 \pm 0.2) 10^7 \text{ s}^{-1} \quad \text{and} \quad \Delta = 13.7 \pm 0.8 \text{ K},$$

$$\tau_0^{-1} = (2.1 \pm 0.9) 10^7 \text{ s}^{-1} \quad \text{and} \quad \Delta = 16.9 \pm 2.4 \text{ K}.$$

Figure 8 shows a comparison between the fittings corresponding to the Mössbauer and susceptibility data. In the range from 1.9 to 2.8 K,³ the latter gives

$$\tau_0^{-1} = (5.4) 10^6 \text{ s}^{-1} \quad \text{and} \quad \Delta = 22.2 \text{ K}. \quad (5.11)$$

The differences between the Mössbauer and susceptibility fitted data can be explained in part as follows. The simple Arrhenius law assumes a potential barrier whose magnitude is independent of the temperature. Actually, as the temperature increases, spin states with greater and greater energy become populated. Therefore, the magnitude barrier that has to be overcome decreases as the temperature increases. Thus it is not surprising that the Mössbauer data, which were collected between 4 and 18 K, give a value for Δ that is smaller than that determined from susceptibility measurement. Moreover, since τ_0^{-1} increases with the transition probabilities per unit time, τ_0^{-1} is also expected to increase with the temperature.

ACKNOWLEDGMENTS

We wish to thank Dr. A. Cornia, Professor D. Gatteschi, Dr. R. Sessoli, and Dr. L. Sorace for many fruitful discussions about this work. Also, we wish to thank EC through MOLNANOMAG (Contract No. HPRN-CT-00012) and INFN-PRA for their financial support.

APPENDIX

Let us start from the equation expressing the temporal evolution of I :

$$I(t) = \exp(iH^x t) I(0). \quad (A1)$$

Passing to the Laplace transform $I(p)$ of $I(t)$,

$$I(p) = \int_0^\infty dt \exp(-pt) I(t), \quad (A2)$$

we have

$$I(0) = (p - iH^x) I(p). \quad (A3)$$

Now, let us introduce the operator P defined by

$$PO = \text{Tr}\{\rho_b O\}_b = \langle O \rangle_b, \quad (A4)$$

where O is an operator which depends on both spin and thermal-bath variables. Since $P^2 = P$ and $P(P-1) = 0$, P is a projecting operator on the spin space.

By applying, first P and then $1-P$ to both sides of Eq. (A3), posing $I(p) = I_1(p) + I_2(p)$ with $I_1(p) = PI(p)$ and $I_2(p) = (1-P)I(p)$, and, lastly, eliminating $I_2(p)$ from the equations, we obtain

$$\begin{aligned} \{p - iPH^x + PH^x[p - i(1-P)H^x]^{-1}(1-P)H^x\} I_1(p) \\ = I(0). \end{aligned} \quad (A5)$$

Let us define

$$R(p) = PH^x[p - i(1-P)H^x]^{-1}(1-P)H^x. \quad (A6)$$

We write $H^x = H_1^x + H_2^x + H_{12}^x$, and take into account that $PH_1^x O = H_1^x P O$, whatever O may be, and $PH_2^x O = 0$, as follows from the relation $PH_2^x O = P(H_2 O - O H_2) = 0$. Then, by considering the equality

$$[p - i(1-P)H^x]^{-1} = p^{-1} \left\{ 1 + \sum_n \left(\frac{i}{p} \right)^n [(1-P)H^x]^n \right\}, \quad (A7)$$

it can easily be seen that $R(p)$ can be rewritten in the form

$$R(p) = PH_{12}^x (1-P) [p - i(1-P)H^x]^{-1} (1-P) H_{12}^x P, \quad (A8)$$

and, finally,

$$I_1(p) = [p - iH_1^x + R(p)]^{-1} I(0). \quad (A9)$$

From this equation, we see that the effects of the interaction with the thermal bath on the spin cluster are described by an operator R . Moreover, the quantum tunneling is described by H_1 . To be more precise, for the cluster ground state we can write $H_1 = H_1^{(0)} + H_{eff}$, where $H_1^{(0)}$ is the unperturbed Hamiltonian, the states of which are the six lowest Kramer's doublets and the nine highest singlets. H_{eff} , by coupling the two states of each doublet, causes the quantum tunneling to occur.

Now let us consider the Laplace transform $f(p)$ of the correlation function of the magnetization, which can be written in the form

$$\begin{aligned} f(p) &= \langle I(0) [p - iH_1^x + R(p)]^{-1} I(0) \rangle \\ &= \sum_{M, M'} \rho_M M M' \langle M, M | [p - iH_1^x + R(p)]^{-1} | M', M' \rangle. \end{aligned} \quad (A10)$$

In order to determine the matrix elements $\langle M, M | [p - iH_1^x + R(p)]^{-1} | M', M' \rangle$, we first have to build the matrix of $[p - iH_1^x + R(p)]$, and then take the inverse of it. As shown in Ref. 16, the only relevant matrix elements of $[p - iH_1^x + R(p)]$ are the ones between Liouville states $|M, M'\rangle$, for which the energies $E_M = E_{M'}$ are equal. For these elements, we have

$$\begin{aligned} \langle M_1, M'_1 | [p - iH_1^x + R(p)] | M_2, M'_2 \rangle \\ = \langle M_1, M'_1 | [p - iH_{eff}^x + R(p)] | M_2, M'_2 \rangle. \end{aligned} \quad (A11)$$

At this point, we will express $R(p)$ in terms of W 's. Since H_{12} is small with respect to the energy difference between the spin states, we can perform the calculation, at the lowest order in the perturbation theory, by writing¹⁷

$$\begin{aligned} R(p) = PH_{12}^x(1-P) \int_0^\infty dt \exp[-pt + i(H_1^{(0)x} + H_2^x)t] \\ \times (1-P)H_{12}^xP. \end{aligned} \quad (A12)$$

As $H_{12} = FA(S_x, S_y, S_z)$, we have $(1-P)H_{12}^xPO = (F - \langle F \rangle_b)[A, \langle O \rangle_b]$, and assuming $\langle F \rangle_b = 0$ we obtain $(1-P)H_{12}^xPO = FA^xPO$. Taking this relation into account, we can rewrite $R(p)$ in the form

$$R(p) = \int_0^\infty dt \exp(-pt) \langle F(0)F(t) \rangle A^x \exp(H_1^{(0)x}t) A^x. \quad (A13)$$

Since operator A does not couple the states of the doublets, it is sufficient that we consider the R matrix elements within the set of states $\{|M_i, M_i\rangle\}$. We have

$$\begin{aligned} \langle M_i, M_i | A^x \exp(H_1^{(0)x}t) A^x | M_j, M_j \rangle \\ = \sum_{k,l} (\langle M_i | A | M_k \rangle \delta_{il} - \langle M_i | A | M_l \rangle \delta_{ik}) (\langle M_k | A | M_j \rangle \delta_{jl} \\ - \langle M_l | A | M_j \rangle \delta_{jk}) \exp(i\omega_{kl}t), \end{aligned} \quad (A14)$$

where $\omega_{kl} = (E_{M_k} - E_{M_l})/\hbar$. From this the following relations follow:

$$\begin{aligned} \langle M_i, M_i | A^x \exp(H_1^{(0)x}t) A^x | M_j, M_j \rangle \\ = \begin{cases} 2 \operatorname{Re} \sum_k A_{ik}^2 \exp(i\omega_{kit}) & \text{per } i=j \\ -2 \operatorname{Re} A_{ij}^2 \exp(i\omega_{kit}) & \text{per } i \neq j \end{cases} \end{aligned} \quad (A15)$$

where $A_{rs} = \langle M_r | A | M_s \rangle$

We wish now to show that, to a good approximation, $R(p) \approx R(0)$. In order to prove this, by assuming for $\langle F(0)F(t) \rangle$ an exponential trend with τ_0 as the correlation time, according to Eqs. (A13) and (A15), we can write, for $i \neq j$,

$$\langle M_i, M_i | R(p) | M_j, M_j \rangle \approx -2A_{ij}^2 F^2 \operatorname{Re} \left(\frac{1}{p + \tau_0^{-1} + i\omega_{ij}} \right). \quad (A16)$$

Since we assumed $\tau_0^{-1} \gg \omega_{ij}$, with all the more reason also $F\tau_0 \ll 1$. As order of magnitude, we then have

$$R \approx F(F\tau_0) \frac{1}{1 + p\tau_0} = F(F\tau_0) \left(1 - \frac{p\tau_0}{1 + p\tau_0} \right). \quad (A17)$$

The p -dependent term of this equation differs from p for the quantity $(F\tau_0)^2/(1 + p\tau_0)$, which, for our assumptions, is much smaller than 1. That is, the terms $p + R(p)$ in Eq. (A11) can be replaced by $p + R(0)$. Finally, the nondiagonal matrix elements of $R(0)$ are given by

$$\begin{aligned} \langle M_i, M_i | R(0) | M_j, M_j \rangle &= -A_{ij}^2 \int_{-\infty}^\infty dt \langle F(0)F(t) \rangle \\ &= -W_{M_i, M_j}, \end{aligned} \quad (A18)$$

and the diagonal matrix elements by

$$\begin{aligned} \langle M_i, M_i | R(0) | M_i, M_i \rangle &= \sum_{k(k \neq i)} A_{ik}^2 \int_{-\infty}^\infty dt \langle F(0)F(t) \rangle \\ &= \sum_{k(k \neq i)} W_{M_i, M_k}. \end{aligned} \quad (A19)$$

As far as the matrix elements of H_{eff} are concerned, the non-null ones are (Fig. 3)

$$\begin{aligned} \langle M, M | H_{eff}^x | -M, M \rangle &= \langle -M, M | H_{eff}^x | M, M \rangle = \nu_M, \\ \langle M, M | H_{eff}^x | M, -M \rangle &= \langle M, -M | H_{eff}^x | M, M \rangle = -\nu_M, \end{aligned} \quad (A20)$$

where ν_M is the quantum tunneling frequency for the spin state M .

¹C. Delfs, D. Gatteschi, L. Pardi, R. Sessoli, K. Wieghardt, and D. Hanke, *Inorg. Chem.* **32**, 3099 (1993).

²A. L. Barra, A. Caneschi, A. Cornia, F. Fabrizi de Biani, D. Gatteschi, C. Sangregorio, R. Sessoli, and L. Sorace, *J. Am. Chem. Soc.* **121**, 5302 (1999).

³A. L. Barra, P. Debrunner, D. Gatteschi, Ch. E. Schultz, and R. Sessoli, *Europhys. Lett.* **35**, 133 (1996).

⁴A. Bouwen, A. Caneschi, D. Gatteschi, E. Goovaerts, D. Schöemaker, L. Sorace, and M. Stefan, *J. Phys. Chem. B* (to be published).

⁵A. L. Barra, D. Gatteschi, and R. Sessoli, cond-mat/0002386 (unpublished). Also see <http://xxx.lanl.gov/html/cond-mat/0002386>

⁶R. Caciuffo, G. Amoretti, A. Murani, R. Sessoli, A. Caneschi, and D. Gatteschi, *Phys. Rev. Lett.* **81**, 4744 (1998).

- ⁷G. Amoretti, S. Carretta, R. Caciuffo, H. Casalta, A. Cornia, M. Affronte, and D. Gatteschi, *Phys. Rev. B* (to be published).
- ⁸C. Sangregorio, T. Ohm, C. Paulsen, R. Sessoli, and D. Gatteschi, *Phys. Rev. Lett.* **78**, 4645 (1997).
- ⁹W. Wernsdorfer and R. Sessoli, *Science* **284**, 133 (1999).
- ¹⁰W. Wernsdorfer, R. Sessoli, A. Caneschi, D. Gatteschi, and A. Cornia, *Europhys. Lett.* **50**, 552 (2000).
- ¹¹H. J. Zeiger and G. W. Pratt, *Magnetic Interaction in Solids* (Clarendon Press, Oxford, 1973), p. 546.
- ¹²A. Caneschi, L. Cianchi, F. Del Giallo, D. Gatteschi, P. Moretti, F. Pieralli, and G. Spina, *J. Phys.: Condens. Matter* **11**, 3395 (1999).
- ¹³A. Abragam, *Les Principes du Magnétisme Nucléaire* (Presses Universitaires de France, Paris, 1961).
- ¹⁴R. Kubo, M. Toda, and N. Kashitsume, *Statistical Physics II* (Springer-Verlag, Berlin, 1985).
- ¹⁵L. Cianchi, P. Moretti, M. Mancini, and G. Spina, *Rep. Prog. Phys.* **49**, 1243 (1986).
- ¹⁶M. Mancini, G. Spina, L. Fiesoli, L. Cianchi, and P. Moretti, *Phys. Rev. B* **25**, 100 (1982).
- ¹⁷R. Zwanzig, *Physica (Amsterdam)* **30**, 1109 (1964).